

MAMBO 1.25 mm observations of 3CR quasars at $z \sim 1.5$: on the debate of the unified schemes

M. Haas¹, R. Chini¹, S. A. H. Müller¹, F. Bertoldi², and M. Albrecht³

¹ Astronomisches Institut, Ruhr-Universität Bochum (AIRUB), Universitätsstr. 150 / NA7, 44780 Bochum, Germany
e-mail: haas@astro.rub.de

² Radioastronomisches Institut, Universität Bonn, Auf dem Hügel 71, 53121 Bonn, Germany

³ Instituto de Astronomía, Universidad Católica del Norte, Avenida Angamos 0610, Antofagasta, Chile

Received 16 December 2004 / Accepted 2 September 2005

ABSTRACT

In order to explore the nature of the $850\mu\text{m}$ flux difference between powerful radio galaxies and steep radio-spectrum quasars at $z \sim 1.5$ reported by Willott et al. (2002), we have observed 9 sources from their sample of 11 quasars at 1.25 mm. For 7 sources the 1.25 mm fluxes are much brighter than one would expect from a purely thermal dust model fitted to the submm data, providing evidence for the synchrotron nature of the observed 1.25 mm radiation. If we extrapolate a power-law synchrotron spectrum to shorter wavelengths, then for 6 of the 9 sources also the $850\mu\text{m}$ fluxes are dominated by synchrotron radiation. We discuss how far the (sub)-millimetre data can be interpreted in accordance with the orientation-dependent unified schemes for powerful radio galaxies and quasars. In this case the results challenge the reported evidence for the receding torus model and for the evolutionary trend of a declining dust luminosity with increasing projected size of the radio lobes.

Key words. galaxies: fundamental parameters – galaxies: photometry – galaxies: quasars: general – infrared: galaxies

1. Introduction

Here we consider two observational AGN classes, the FR2 radio galaxies and the steep radio-spectrum quasars, both with *powerful* edge-brightened radio lobes ($P_{408\text{ MHz}} \gtrsim 10^{24.5} \text{ W Hz}^{-1}$). According to the orientation-dependent unified schemes both classes are believed to belong to the same parent population with the observed differences being just a consequence of their viewing angle: the jet axis of quasars is more aligned with our line of sight than that of radio galaxies (Orr & Browne 1982) and the nuclear region of radio galaxies is hidden behind a dusty torus seen roughly edge-on (Barthel 1989). For these idealised versions of the unified schemes two predictions can be tested observationally: firstly, at mm wavelengths the beamed synchrotron radiation should be higher in the quasars than in the radio galaxies. Secondly, the isotropic far-infrared dust emission of radio galaxies should be similar to that of quasars at matched isotropic radio lobe power.

Both predictions have been confirmed for 3CR sources at $z \lesssim 1.5$ by means of sensitive ISO mid- and far-infrared and IRAM millimetre observations: For ten radio galaxy – quasar pairs matched in 178 MHz power Meisenheimer et al. (2001) found a similar dust detection statistics as well as a higher synchrotron contribution in quasars. For a sample of eight sources van Bemmelen & Bertoldi (2001) inferred also a higher synchrotron contribution in quasars. Using the full set of ISO FIR observations of 75 sources Haas et al. (2004) found

corroborating evidence for the orientation-dependent unified schemes.

At redshift $z \gtrsim 1.5$ the restframe FIR dust emission begins to shift into the submillimetre wavelength range. Based on SCUBA observations of 23 sources at $1.3 < z < 1.9$ Willott et al. (2002) found that the quasars have a higher $850\mu\text{m}$ flux than the radio galaxies. They argue that the $850\mu\text{m}$ flux of these $z \sim 1.5$ quasars is dominated by dust emission and not by synchrotron radiation. If this were true, such a dust luminosity difference between quasars and radio galaxies would not be consistent with a simple version of the orientation-dependent unified schemes. However, the thermal nature of the observed $850\mu\text{m}$ fluxes has still to be established. In fact, the non-thermal synchrotron and free-free contribution in these sources is not known. In the following we consider only thermal and synchrotron emission, since the data bases are too sparse to separate the observed fluxes into three components and free-free emission generally plays a minor role in radio-loud AGN; if significant, then free-free emission would not only reduce the synchrotron, but also the thermal component.

In order to explore the nature of the $850\mu\text{m}$ emission, 1.25 mm (or 3 mm) photometry allows to estimate the synchrotron contribution at mm wavelengths and to extrapolate it to the submm range. Therefore, we observed the 9 brightest quasars of Willott et al.'s sample, which provided the highest likelihood of achieving a detection at 1.25 mm with the Max-Planck millimetre bolometer array MAMBO (Kreysa et al. 1998).

Table 1. Fluxes and other parameters of the quasar sample. The total submm fluxes are from Willott et al. (2002), observed between March 1999 and April 2001. Column 7 lists the thermal contribution at 1.25 mm derived from a dust model fitted to the submm data, as explained in Sect. 3.1.1 and shown in Fig. 2. Column 8 lists the synchrotron contribution at 1.25 mm, as total minus thermal contribution (Cols. 3–7) and Col. 9 lists the synchrotron fraction in percent. The spectral indices $\alpha_{\text{cm-mm}}$ are determined for most sources between 6 cm and 1.25 mm with an accuracy of better than 5%; more details are given in Sect. 3.1.2. These spectral indices are used to extrapolate from longer wavelength data the 450 and 850 μm synchrotron fluxes listed in Cols. 11 and 12.

(1)	(2)	(3)	(4)	(5)	(6)	(7)	(8)	(9)	(10)	(11)	(12)
Object	z	$F_{1.25\text{ mm}}$ [mJy]	observ. date	$F_{850\ \mu\text{m}}^{\text{total}}$ [mJy]	$F_{450\ \mu\text{m}}^{\text{total}}$ [mJy]	$F_{1.25\ \text{mm}}^{\text{thermal}}$ [mJy]	$F_{1.25\ \text{mm}}^{\text{syn}}$ [mJy]	syn [%]	$\alpha_{\text{cm-mm}}$	$F_{850\ \mu\text{m}}^{\text{syn}}$ [mJy]	$F_{450\ \mu\text{m}}^{\text{syn}}$ [mJy]
3C 181	1.382	5.96 ± 1.11	17.10.04	5.27 ± 1.06	-0.8 ± 7.5	0.66	5.30	88	-1.23	3.73	
3C 191	1.952	5.36 ± 1.24	17.10.04	6.39 ± 1.06	28.9 ± 8.1	1.04	4.32	80	-1.17	3.44	1.63
3C 205	1.534			2.36 ± 1.10	11.6 ± 7.9				-1.35 ^b	2.24 ^b	
3C 268.4	1.400	8.53 ± 1.56	16.10.04	5.13 ± 1.18	9.9 ± 12.5	1.11	7.42	86	-1.10	5.55	
3C 270.1	1.519	11.92 ± 2.69	02.06.04	7.42 ± 1.17	15.4 ± 11.5	1.07	10.85	91	-1.11	7.76	3.83
3C 280.1	1.659	3.99 ± 1.24	16.10.04	5.10 ± 1.74	0.4 ± 23.8	<1.31 ^a	>2.68 ^a	67	-1.15	2.62	
3C 298	1.439	20.68 ± 3.68	02.06.04	21.13 ± 2.06	-8.0 ± 23.7	2.12	18.56	89	-1.10	13.88	
3C 318	1.574	5.61 ± 1.42	02.06.04	7.78 ± 1.00	21.6 ± 10.6	0.99	4.62	82	-1.32	3.53	
3C 432	1.785	0.34 ± 1.54	29.05.04	7.93 ± 1.70	2.9 ± 20.9	2.06	<2.56	55	-1.25 ^b	1.60 ^b	
4C 38.30	1.405			-0.01 ± 1.11	8.9 ± 7.8				-1.10 ^b	1.14 ^b	
4C 35.23	1.594	11.93 ± 2.89	02.06.04	9.18 ± 1.10	21.3 ± 6.8	0.68	11.25	94	-0.89	8.60	4.88

^a Upper and lower limits adopted, because the thermal model is constrained by submm upper flux limits only.

^b Determined/extrapolated from the cm wavelength range only.

2. Observations and data

The MAMBO 1.25 mm (250 GHz) continuum observations were performed at the IRAM 30-m telescope during the pooled observation campaigns between May and October 2004. We used the standard on-off photometry observing mode, chopping between the target and sky at 2 Hz, and nodding the telescope every 10 s. The atmospheric transmission was intermediate with $\tau(1.2\text{ mm})$ between 0.15 and 0.5. The absolute flux calibration was established by observations of Mars and Uranus, resulting in a flux calibration uncertainty of about 20%. The data were reduced using the MOPSI software package.

The 1.25 mm fluxes are listed in Table 1, together with the submm fluxes and other parameters discussed below. Figure 1 shows the spectral energy distributions (SEDs), with the submm-mm range being zoomed in Fig. 2. At a redshift $z \geq 1.5$ the host galaxies are unresolved. The 1.25 mm fluxes refer to a beam size of 11'' of the IRAM 30m telescope, which is similar to the JCMT-SCUBA 850 μm beam of 15'', but smaller than the size of the extended radio structures measured at cm wavelengths. Any extended contribution to the submm and mm fluxes, if significant at all, may be missed, but we will see below (Sect. 3.1.2) that this effect might be negligible.

3. Results and discussion

We investigate our quasar 1.25 mm data and their implications on the nature of the 850 μm emission. In order to test the unified schemes, we then compare the quasars with radio galaxies.

3.1. Quasars

This section is sub-divided into three steps: (1) in order to determine the nature of the 1.25 mm fluxes we firstly consider the extreme case adopting that the submm fluxes are entirely thermal; (2) since we find that for most sources the 1.25 mm fluxes are dominated by synchrotron radiation, we explore its influence on the nature of the 850 μm fluxes; (3) finally we consider the remaining evidence for thermal 850 μm emission.

3.1.1. Synchrotron nature of the 1.25 mm fluxes

The most striking result from Fig. 2 is the strong evidence that the 1.25 mm data are much brighter than one would expect from a purely thermal dust model fitted to the submm data.

For the first step we assume that the submm fluxes are entirely due to dust emission. With a dust emissivity $\beta = 2$ a greybody fit to the 450 and 850 μm data yields a dust temperature in the range $40\text{ K} < T < 60\text{ K}$ for all sources, except 4C 35.23 discussed below. Because of the numerous 450 μm upper limits the individual temperature values are quite uncertain. Therefore, for all sources we use $T = 50\text{ K}$ typically found for quasars with high far-infrared and submm luminosity above $10^{12} L_{\odot}$ (e.g. Willott et al. 2002; Haas et al. 2003, 2004). Figure 2 shows the SEDs zoomed around the submm-mm data and a modified blackbody at $T = 50\text{ K}$; the strength of this greybody is constrained by the 450 μm data points for all sources except 3C 280.1, for which the 450 μm upper limit is rather high and we used the 850 μm constraint.

For 4C 35.23 the greybody fit to the 450 and 850 μm data results in a low dust temperature $T \approx 20\text{ K}$; since this is an

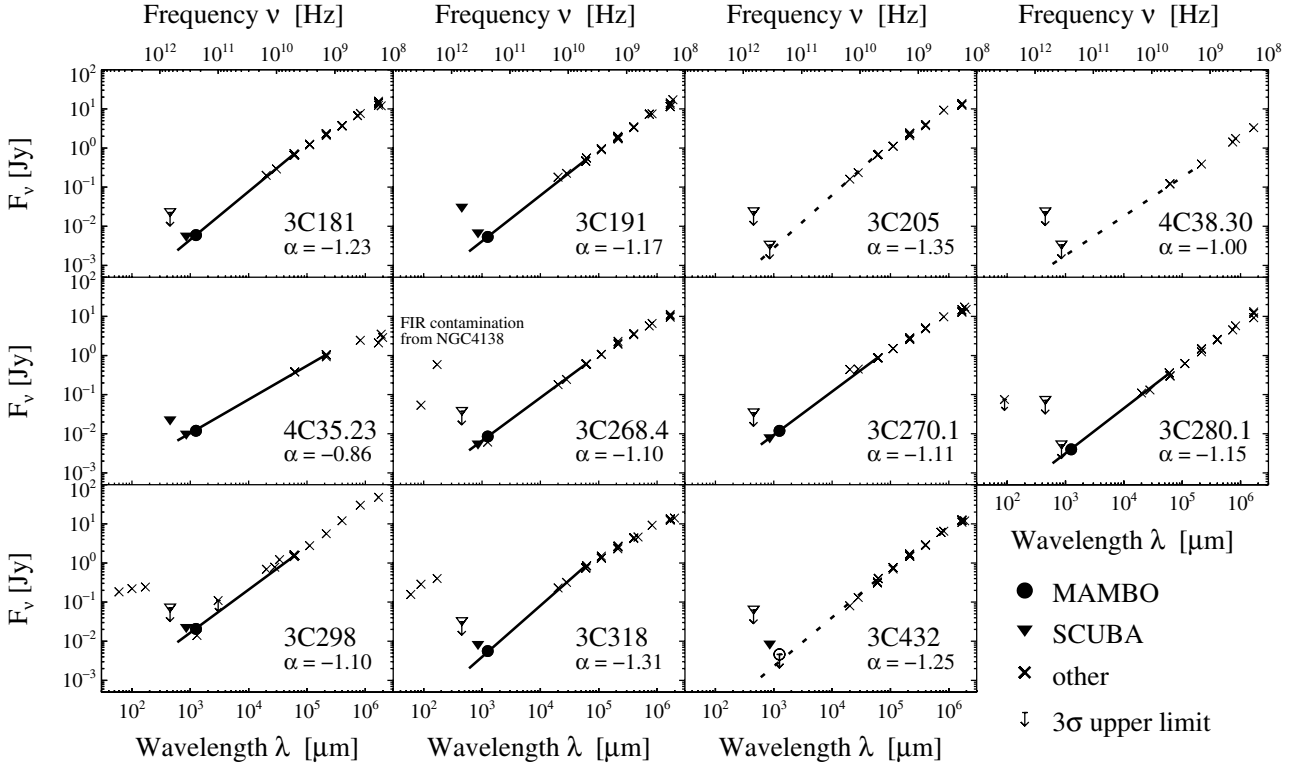


Fig. 1. Observed SEDs of the quasars. The errors are smaller than the size of the symbols; open symbols with arrows represent 3σ upper limits. The drawn straight lines show the synchrotron spectrum from the cm to the mm wavelength range with spectral index α ($=\alpha_{\text{cm-mm}}$ in Table 1); these lines are dotted in case of an upper limit or a missing data point at 1.25 mm. As already noted by Haas et al. (2004) the exceptionally high FIR 90 and 170 μm fluxes of 3C 268.4 reported by Andreani et al. (2002) are contaminated by the nearby galaxy NGC 4138.

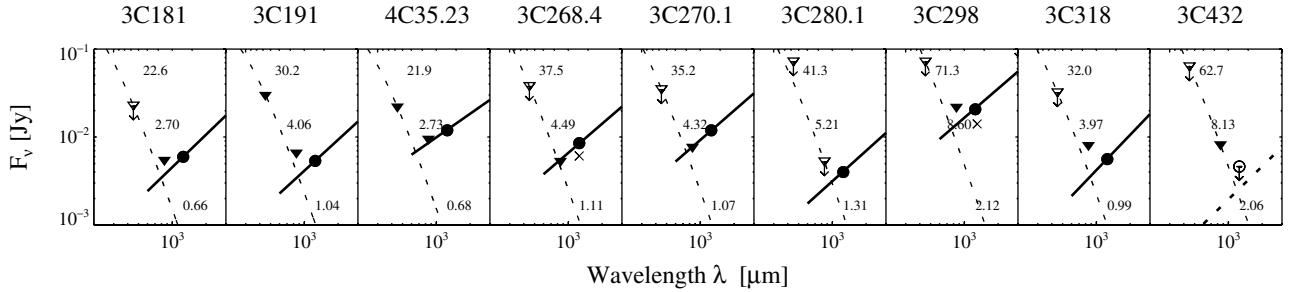


Fig. 2. SEDs of the nine quasars observed at 1.25 mm, zoomed around the submm-mm data points. The errors are in the order of the size of the symbols. The symbols are as in Fig. 1. The dotted lines show a 50 K modified blackbody (emissivity $\beta = 2$) with three numbers in each panel listing its flux values at 450, 850 and 1250 μm ; the strength of this greybody is constrained by the 450 μm data for all sources except for 3C 280.1 for which it is constrained by the 850 μm upper limit. The plots clearly illustrate the non-thermal nature of the 1.25 mm fluxes for at least seven sources, the exceptions are 3C 432 and perhaps also 3C 280.1. The drawn straight lines show the synchrotron spectrum as in Fig. 1.

extremely unusual value for such an active high-luminosity object, and since the 850 μm data point lies nicely on the synchrotron extrapolation (as shown in Fig. 2 and discussed further below), this argues in favour of the warmer, say $T \approx 50$ K, dust component running through the 450 μm data point only. Even more extreme, the attempt to fit the 850 μm and 1.25 mm data by a greybody results in exceptionally low temperatures, for example $T \approx 9$ K for 3C 191 and 3C 318, and even much lower for the other sources (except 3C 432). Since we hesitate to postulate the existence of such a cold bright dust component in luminous quasars, we conclude that the 1.25 mm fluxes

are mainly due to synchrotron radiation. Table 1 lists the thermal 1.25 mm contribution derived from the $T = 50$ K blackbody shown in Fig. 2, as well as the 1.25 mm synchrotron contribution as difference of total minus thermal 1.25 mm flux. For at least seven quasars (i.e. all except 3C 280.1 and 3C 432) the synchrotron fraction lies above $\sim 80\%$ of the total 1.25 mm flux. Considering the errors, if we adopt the extreme case that all actual 1.25 mm fluxes are 20% lower, then for seven sources the synchrotron fraction still remains above $\sim 75\%$. This fraction becomes higher, if we do not assume that the submm fluxes are of thermal nature.

In the discussion here, we do not make use of a possible synchrotron variability between different observing dates, since suitable monitoring data are not available for the entire sample. Two sources, notably, have been observed also at 1.25 mm on other dates: 3C 298 (14.1 ± 0.8 mJy in Dec. 1998, Meisenheimer et al. 2001) and 3C 268.4 (6.1 ± 1.0 in March 1996, Andreani et al. 2002). Compared with our data taken in summer/autumn 2004 (Table 1) some variability may be present, for 3C 298 also indicated by the irregular deviation of the cm flux values from a straight line (Fig. 2 in Willott et al. 2002). In these two cases, however, any variability appears to be moderate ($\lesssim 30\%$) and lies within the calibration and measurement errors.

3.1.2. Synchrotron contribution at $850\ \mu\text{m}$

The high 1.25 mm synchrotron fraction suggest that also the $850\ \mu\text{m}$ fluxes may contain a high synchrotron contribution. Notably, in this case our initial assumption on the purely thermal nature of the submm fluxes would be invalidated, further reinforcing the synchrotron nature of the 1.25 mm emission concluded above.

The precise extrapolation of the 1.25 mm synchrotron contribution to shorter wavelengths depends on the shape and slope of the synchrotron spectrum. Thereby two aspects are important:

- 1) As discussed by Willott et al. (2002) and references therein a study of several steep radio-spectrum sources between 22 GHz and 230 GHz shows that the radio *cores* are the essential contributors to the 1.25 mm and $850\ \mu\text{m}$ synchrotron fluxes. The cores have a typical spectrum $F_\nu \propto \nu^\alpha$ with, on average, $\alpha \sim -1$. Applying this average α value for the extrapolation of the 1.25 mm data to shorter wavelengths clearly results in high $850\ \mu\text{m}$ synchrotron contributions which, however, could be caused by the scatter of α . Therefore we try to obtain better estimates for the individual sources. Due to the lack of sufficient radio *core* data of our sources we here investigate their *total* spectra.
- 2) In principle, there may be a spectral break at wavelengths between 1.25 mm and $850\ \mu\text{m}$ (for both core and total spectra). To our knowledge, however, such an extreme break, occurring within a factor of only 1.5 in frequency range, has not yet been observed so far. Also, according to theoretical models such a break should show up already via a deviation from the power-law shape extending over at least a factor of ten in frequency, i.e. a pronounced downward curvature of the spectrum between cm and mm wavelengths (e.g. Pacholzyk 1980, see Fig. 3 in Marscher 1977 and Fig. 1 in Crusius & Schlickeiser 1986). In order to check for such a curvature, additional 3 mm data would be ideal, but they are not available for our sources. Therefore, we here investigate the present cm-mm spectra.

The aim now is to check for signatures of a curvature between cm and mm wavelengths, which would indicate a spectral break between 1.25 mm and $850\ \mu\text{m}$ and, if such signatures are not found, to get an estimate on the $850\ \mu\text{m}$ synchrotron contribution via power-law extrapolation from the 1.25 mm data points.

In order to facilitate the following analysis we start with the assumption that the 1.25 mm fluxes are entirely due to synchrotron emission. In a first step we visually fitted the spectral indices α at wavelengths $2\ \text{cm} \lesssim \lambda \lesssim 21\ \text{cm}$. Drawing these lines further down to mm wavelengths results in extrapolated 1.25 mm fluxes close to those observed. In a refined second step we fitted the spectral indices including also the 1.25 mm data. The exact wavelength range used depends on the available data. In general $\alpha_{\text{cm-mm}}$ was determined between 6 cm and 1.25 mm; slightly different wavelength ranges were used for 3C 205 (6 cm–2 cm), 4C 38.30 (21 cm–2 cm), and 4C 35.23 (21 cm–1.25 mm), yielding $\alpha_{\text{cm-mm}}$ values similar to those of the other sources. The spectral indices $\alpha_{\text{cm-mm}}$ lie between -0.9 and -1.35 , a range also found for quasars and BLRGs by van Bemmell & Bertoldi (2001). While we had to choose slightly different cm wavelength ranges, the inclusion of the 1.25 mm data point makes the fit of $\alpha_{\text{cm-mm}}$ very stable with uncertainties below 2%. For the two cases without mm data we used the shortest cm spectral range which follows a power-law, and we estimate the formal fit uncertainty of α to be less than 5% which is negligibly small compared with the influence of other effects like variability or a possible spectral curvature between cm and mm wavelengths.

The fact that the 1.25 mm data points lie on (or very close to) the power-law extrapolation of the radio cm spectra to shorter wavelengths (Fig. 1) suggests that any spectral curvature around 1 mm is weak, hence that there is no strong spectral break between 1.25 mm and $850\ \mu\text{m}$. Also, it indicates that probably not much extended mm flux is missed as mentioned above (Sect. 2), thereby arguing in favour of the synchrotron nature of the 1.25 mm fluxes, too. Both results are also valid, if we modify the assumption that (instead of 100%) only 75–80% of the 1.25 mm fluxes are synchrotron radiation.

Since the synchrotron spectra follow the $F_\nu \propto \nu^\alpha$ extrapolation from the cm fluxes to shorter wavelengths and show neither any hint for an abrupt break nor a strong curvature, we suggest that the synchrotron contribution at $850\ \mu\text{m}$ can be extrapolated reasonably well from the 1.25 mm data points using these spectral indices $\alpha_{\text{cm-mm}}$. Noteworthy, $\alpha_{\text{cm-mm}}$ determined from the total spectra is steeper than the average core value $\alpha \sim -1$ (except for 4C 35.23); this suggests that a spectral break between 1.25 mm and $850\ \mu\text{m}$, if any, is even weaker. Therefore, compared with using $\alpha \sim -1$ mentioned above, one may expect that the total $\alpha_{\text{cm-mm}}$ yields a lower than actual $850\ \mu\text{m}$ synchrotron contribution. This contribution (Table 1) already constitutes at least 50% of the observed total $850\ \mu\text{m}$ flux for five sources (3C 181, 3C 191, 3C 280.1, 3C 298, 3C 318) and reaches about 100% for three sources (3C 268.4, 3C 270.1, 4C 35.23); only for one source (3C 432) it lies at about 20%. Also for the two sources without 1.25 mm data, the tentative extrapolation of the cm spectra yields a $850\ \mu\text{m}$ synchrotron fraction of $\geq 30\%$ (4C 38.30) and 100% (3C 205). Thus, as long as future data do not reveal a synchrotron break between 1.25 mm and $850\ \mu\text{m}$, we conclude that in most (9/11) sources not only the 1.25 mm fluxes, but also the $850\ \mu\text{m}$ fluxes are dominated by synchrotron radiation.

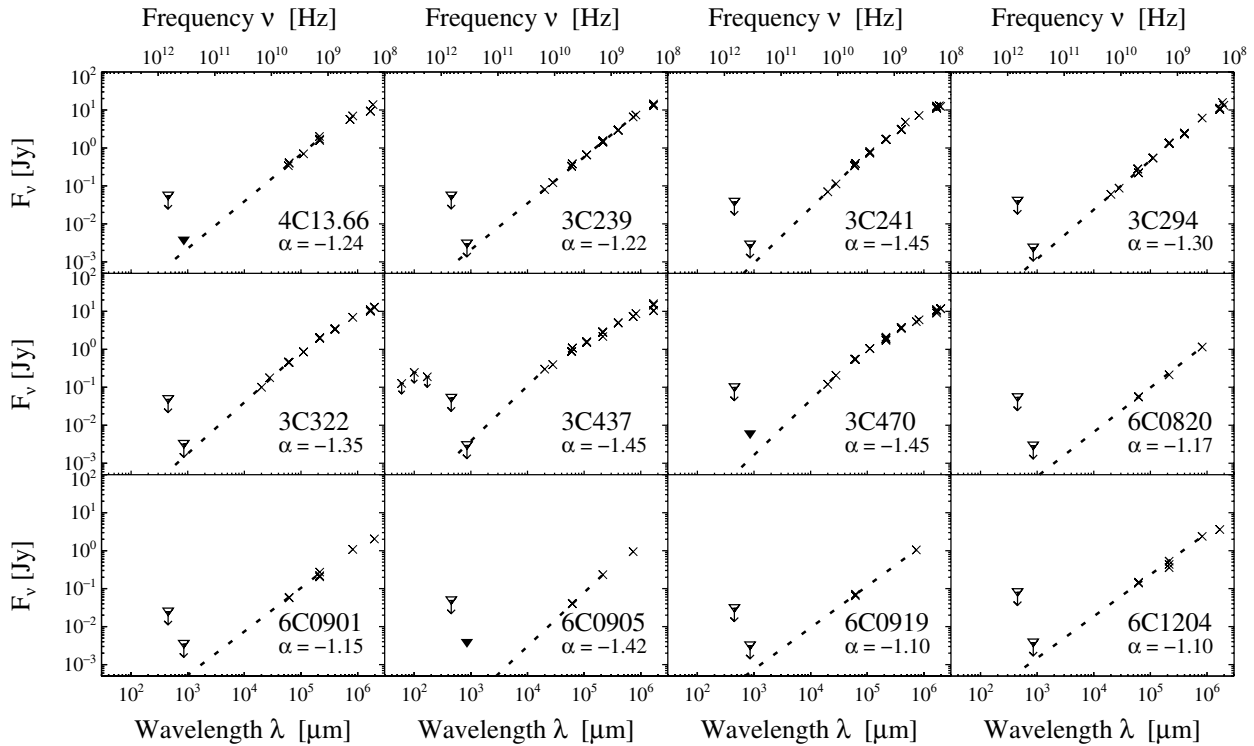


Fig. 3. Observed SEDs of the comparison radio galaxies. Symbols are as in Fig. 1.

3.1.3. Thermal contribution at $850\mu\text{m}$

Although one could fit a combined model consisting of a thermal and a synchrotron component to the SEDs, we do not present nice fits here because they do not provide further insight and bear the risk of diluting the attention for the implicit assumptions made; instead we prefer to extract the conclusions from considering various cases with clear assumptions.

Again, we assume in a first step a 100% synchrotron nature of the 1.25 mm fluxes and extrapolate the $850\mu\text{m}$ synchrotron contribution using $\alpha_{\text{cm-mm}}$ derived from the total sources. In order to determine which sources still show evidence for thermal $850\mu\text{m}$ emission, from the entire $850\mu\text{m}$ fluxes we subtract the synchrotron contribution.

From inspection of Figs. 1 and 2 and with values listed in Table 1 we find only five such quasars out of eleven. Three show evidence for thermal submm emission from data at both 450 and $850\mu\text{m}$ (3C 191, 3C 318, 3C 432), one source (4C 35.23) only from data at $450\mu\text{m}$, and for one source (3C 280.1) the rather high upper submm flux limits may allow for thermal $850\mu\text{m}$ emission. For the other four quasars any evidence for thermal $850\mu\text{m}$ emission remains weak, even if we reduce the 1.25 mm synchrotron fraction from 100% down to 75%; in order to allow for a dominant thermal $850\mu\text{m}$ emission in these sources a strong spectral break between 1.25 mm $850\mu\text{m}$ would be required, but the current data do not show signatures in favour of such a break.

In the two cases without 1.25 mm data (3C 205 and 4C 38.30), the observed $850\mu\text{m}$ upper limits lie only marginally above the synchrotron spectrum extrapolated from the cm wavelengths; thus, considering the entire sample this

would result in six out of eleven quasars showing no evidence for a significant thermal $850\mu\text{m}$ emission.

3.2. Comparison with radio galaxies

In order to test the unified schemes we compare the quasars with the sample of radio galaxies at matched redshift and 151 MHz radio lobe power selected by Willott et al. (2002) and observed by Archibald et al. (2001).

3.2.1. Properties of the radio galaxies

Figure 3 shows the SEDs of the radio galaxies, from the submm to the cm wavelength range, referring to the total fluxes. Suitable mm data are not available for a direct determination of the synchrotron contribution at submm-mm wavelengths. However, we will see below that basic conclusions can be drawn even without such mm data.

For the quasars the power-law fit to the total spectra at cm wavelengths yields synchrotron slopes with values close to those $\alpha_{\text{cm-mm}}$ obtained including also the 1.25 mm data to the fit. Encouraged by this fact we tentatively determine α in the cm regime for the radio galaxies and consider its extrapolation to the mm and submm wavelengths (Fig. 3). As for the quasars, for the radio galaxies we visually fitted the spectral indices α at wavelengths $21\text{ cm} \geq \lambda \geq 2\text{ cm}$. Depending on the available data slightly different wavelength ranges were used for 4C 13.66 and the 6C radio galaxies (21 cm – 6 cm), and for most (4/6) of the 3C galaxies (21 cm – 2 cm). Since two 3C galaxies (3C 437 and 3C 470) show a slight curvature in their cm spectra, i.e. a steepening of the spectra towards shorter wavelengths, we used

Table 2. Parameters of the comparison radio galaxy sample of Willott et al. (2002): Spectral indices, α_{cm} , fitted to the total cm wavelength data with an accuracy of about 5%. Via $F_\nu \propto \nu^\alpha$ the $850\mu\text{m}$ synchrotron fluxes are extrapolated from the cm fluxes with a formal uncertainty of about 30–40%.

Object	z	α_{cm}	$F_{850\mu\text{m}}^{\text{syn}}$ [mJy]
4C 13.66	1.450	-1.24	1.84
3C 239	1.781	-1.22	1.71
3C 241	1.617	-1.45	0.73
3C 294	1.786	-1.30	0.96
3C 322	1.681	-1.35	1.44
3C 437	1.480	-1.45 ^a	3.05
3C 470	1.653	-1.45	1.30
6C 0820+3642	1.860	-1.17	0.37
6C 0901+3551	1.904	-1.15	0.43
6C 0905+3955	1.882	-1.42	0.09
6C 0919+3806	1.650	-1.10	0.62
6C 1204+3708	1.779	-1.10	1.24

^a Actually α_{cm} refers to $\alpha_{\text{cm}-850\mu\text{m}}$, due to the low $850\mu\text{m}$ upper limit.

only the shortest cm range (6 cm–2 cm) to determine their α . In one case (3C 437) the $850\mu\text{m}$ data point indicates a synchrotron spectrum which is even steeper, and we used this steep α value constrained by the $850\mu\text{m}$ data point. Table 2 lists the values for α_{cm} and the extrapolated synchrotron contribution at $850\mu\text{m}$. Because some radio galaxies (e.g. 3C 437 and 3C 470) show the trend of a convex curvature in their cm spectra, for the others one may expect that the α values determined from the cm range actually represent upper limits for the true $\alpha_{\text{cm}-\text{mm}}$; in this case the actual $850\mu\text{m}$ synchrotron contributions will be even lower than the extrapolated values.

Two radio galaxies (3C 470 and 6C 0905) and possibly also a third one (4C 13.66) have a detected total $850\mu\text{m}$ flux lying above this synchrotron extrapolation (Fig. 3, Table 2), hence show signatures for thermal submm emission. Furthermore, in three radio galaxies (6C 0820, 6C 0901 and 6C 0919) the $850\mu\text{m}$ upper flux limits lie clearly above the synchrotron extrapolation, thus in principle allowing for a significant thermal submm contribution, too.

One may ask how far additional 1.25 mm data for the radio galaxies could change this picture. We consider two basic cases assuming that variability, if any, is small:

- 1) If the mm data point would lie so much above the current extrapolation that the evidence for thermal $850\mu\text{m}$ emission disappears (e.g. for 3C 470, 6C 0905), then the synchrotron spectra of the total sources would have a strong upward curvature between cm and mm wavelengths. But in the total spectra of radio galaxies such a strong mm bump has not been observed so far. Also, this possibility was discussed in detail by Archibald et al. (2001, their Sect. 4.2) for those sources in their larger ($z = 0.7$ – 4.4) radio galaxy sample which have radio core data. Even for the worst-case scenario any synchrotron contribution to the $850\mu\text{m}$ core fluxes is negligible ($\lesssim 0.2$ mJy); an exception may be 3C 241

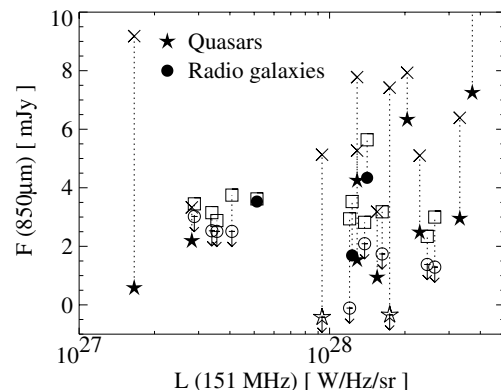


Fig. 4. Distribution of $850\mu\text{m}$ fluxes versus radio lobe luminosities. For each object the total flux and – after subtraction of the synchrotron contribution – the thermal flux is shown, connected by a vertical dotted line. Open symbols with arrows indicate $3\text{-}\sigma$ upper limits. A proper thermal comparison would be via dust luminosities at a given rest-frame wavelength, but would require more data or assumptions on the dust temperature.

likely to have $F_{850\mu\text{m}}^{\text{syn}} \sim 1$ mJy, a value consistent with our extrapolation of $F_{850\mu\text{m}}^{\text{syn}} \sim 0.73$ mJy (Table 2).

- 2) If the mm data point lies below the current extrapolation, then the synchrotron contribution might be even lower and the thermal component higher than derived by our current procedure.

These two considerations suggest that 1.25 mm data are not necessary for drawing the relevant conclusions here. Actually the reason for not obtaining 1.25 mm data for the radio galaxies (and the two faintest quasars) was that at the expected low flux levels $F_{1.25\text{mm}} \lesssim 1$ mJy such observations are very time consuming (≥ 10 h per object).

3.2.2. Comparison of the distributions

The $850\mu\text{m}$ synchrotron contribution for the quasars lies in a range with an average of 4.92 ± 3.82 mJy, which is about a factor of 5 higher and shows a broader distribution than that for radio galaxies (1.15 ± 0.81 mJy). The distributions of spectral slopes $\alpha_{\text{cm}-\text{mm}}$ for quasars and α_{cm} for radio galaxies overlap. The average slopes are -1.16 ± 0.13 and -1.28 ± 0.14 , resp., hence are slightly steeper for the radio galaxies. Both results are consistent with the orientation-dependent unified schemes, where the jet axis of the quasars is thought to be more aligned with our line of sight.

The $850\mu\text{m}$ dust contributions $F_{850\mu\text{m}}^{\text{dust}}$ after subtraction of the synchrotron contribution from the total fluxes are shown in Fig. 4. For three quasars and two radio galaxies $F_{850\mu\text{m}}^{\text{dust}}$ lies above 3 mJy, a value we adopt as observational $3\text{-}\sigma$ detection threshold (Archibald et al. 2001). For six quasars and one radio galaxy, which are detected in total $F_{850\mu\text{m}}$, $F_{850\mu\text{m}}^{\text{dust}}$ falls below this threshold; they would not have been detected without the lift by the synchrotron contribution. Although mainly characterised by upper limits, the averages of $F_{850\mu\text{m}}^{\text{dust}}$ are 2.53 ± 2.45 mJy and 2.21 ± 1.15 mJy for the quasars and radio galaxies, resp.; the higher rms for quasars may be caused by the

subtraction of the larger synchrotron contribution. Thus, from both the number of sources with $F_{850\mu\text{m}}^{\text{dust}} > 3 \text{ mJy}$ and the mean fluxes, any $F_{850\mu\text{m}}^{\text{dust}}$ difference between quasars and radio galaxies is marginal. Again, this is consistent with the orientation-dependent unified schemes, which predict for both AGN classes a similar dust power irrespective of aspect angle.

Actually, the 450 and 850 μm dust contribution of most sources is constrained only by upper limits. A closer look at Table 1 of Willott et al. (2002) shows: While the 850 μm rms is at least as good for the radio galaxy sample as for quasars, at 450 μm the rms of the radio galaxies ($17.3 \pm 6.8 \text{ mJy}$) is worse than that of the quasars ($12.8 \pm 6.7 \text{ mJy}$), indicating that the higher 450 μm detection rate of the quasars may be due to more favourable observing conditions. At 450 μm only two quasars out of 11 are detected at the 3σ level (3C 191 and 4C 35.23). Subtracting the synchrotron extrapolation results in a 450 μm dust contribution which is below the 3σ level for all except one quasar (3C 191). More sensitive FIR observations are required to determine the dust properties of the two samples. As discussed by Haas et al. (2003) for the radio-quiet quasars at $z \gtrsim 1$, the dust temperature may be higher than the usually adopted $T \approx 50 \text{ K}$, so that the emission will still peak at observed FIR wavelengths and not in the sub-mm range.

4. Conclusions

MAMBO 1.25 mm observations of nine 3CR quasars at $z \sim 1.5$ yield the following results:

- 1) For seven sources the 1.25 mm data are much brighter than one would expect from a purely thermal dust model fitted to the submm data. This provides strong evidence that the 1.25 mm fluxes are dominated by synchrotron radiation. Furthermore, in eight of nine cases the 1.25 mm fluxes lie close to the power-law extrapolation $F_\nu \propto \nu^\alpha$ of the total synchrotron spectrum fitted at cm wavelengths, not indicating any pronounced spectral curvature between 2 cm and 1.25 mm.
- 2) The lack of a strong spectral curvature between 1.25 mm and 2 cm, suggests that there is no strong spectral break between 1.25 mm and 850 μm . If the synchrotron contribution at 850 μm is consequently extrapolated from the 1.25 mm data via a power-law $F_\nu \propto \nu^\alpha$, then in at least 6 out of 9 quasars the observed 850 μm fluxes are dominated by synchrotron radiation, too. In this case, only at most five quasars show evidence for substantial thermal 850 μm emission.

In order to test the unified schemes, we compare the quasars with 12 radio galaxies at matched redshift and radio power. As argued by Archibald et al. (2001) from the core spectra of some sources of their larger radio galaxy sample and indicated by our study of the total spectra, the 850 μm synchrotron contribution of the radio galaxies is low. This allows for drawing the following conclusions:

- 1) On average the synchrotron contribution at 850 μm is by a factor of about 5 higher in the quasars and the synchrotron spectral slope is slightly steeper in the radio galaxies,

as expected if the jet axis of the quasars is more aligned with our line of sight.

- 2) After subtraction of the synchrotron contribution we find evidence for thermal 850 μm emission in two (possibly three) detected galaxies, and in three additional galaxies their high 850 μm upper limits allow for dust emission, too. Compared with the quasars, the distribution of the synchrotron subtracted 450 and 850 μm dust emission shows no significant difference to that of the radio galaxies, again consistent with the picture of a similar amount of isotropic dust power irrespective of aspect angle.

As a consequence, as long as future data do not reveal a synchrotron break between 850 μm and 1.25 mm for the quasars or a mm bump for the radio galaxies both being not expected from the current data, the data can be interpreted in accordance with the orientation-dependent unified schemes for powerful radio galaxies and quasars. In this case, our results challenge two speculative conclusions drawn by Willott et al. (2002):

- 1) A luminosity dependent refinement of the unified schemes, the so-called receding torus model (Lawrence 1991), is neither required nor supported by the new data. As argued by Haas et al. (2004), at the high luminosities $P_{408 \text{ MHz}} \gtrsim 10^{24.5} \text{ W Hz}^{-1}$ the scale height of the torus might not be independent of luminosity, rather it may increase due to the impact of supernovae from starbursts accompanying the AGN phenomena. This possibility is also considered by Simpson (2005) who, however, still assumes that the $[\text{O III}]_{500.7 \text{ nm}}$ emission is isotropic. Since this assumption is not correct at high luminosities as shown by Haas et al. (2005) on the basis of *Spitzer* IRS spectra of 3CR sources and the lower $[\text{O III}]_{500.7 \text{ nm}} / [\text{O IV}]_{25.9 \mu\text{m}}$ ratio for galaxies compared with quasars, any remaining evidence for the simple version of the receding torus is further reduced.
- 2) The decline of dust luminosity with the projected linear size – interpreted as age – of the radio source (Fig. 6 in Willott et al. 2002) could be an artefact. Then the trend in this figure might be caused by the higher 850 μm synchrotron contribution in quasars. Of course, evolution of the dust temperature and emission may exist, as was concluded for the optically selected Palomar-Green quasars (Haas et al. 2003), but for the present samples of radio-loud quasars and radio galaxies at $z \sim 1.5$ such evolutionary trends cannot yet be established by the current submm data. Notably, Fanti et al. (2000) already found no evidence that the FIR luminosities of the compact steep spectrum quasars and GHz peaked sources are significantly different from those of the extended objects.

The samples are still small, and the decomposition of the submm and mm data into thermal, synchrotron (and free-free) components are affected by large uncertainties, also due to variability. So far, however, the results from the 1.25 mm data points strongly indicate that Willott et al.'s interpretation of the observed 850 μm difference between quasars and radio galaxies in favour of the receding torus or evolutionary trends should be considered with reservation.

Acknowledgements. It is a pleasure for us to thank IRAM for discretionary observing time with the 30 m telescope at Pico Veleta. For literature and photometry search the NED was used. This work was supported by the Nordrhein-Westfälische Akademie der Wissenschaften. We thank the referee David Hughes for his detailed criticism, and Reinhard Schlickeiser for valuable discussions.

References

- Andreani, P., Fosbury, R., van Bemmell, I., et al. 2002, *A&A*, 381, 389
Archibald, E., Dunlop, J., Hughes, D., et al. 2001, *MNRAS*, 323, 417
Barthel, P. 1989, *ApJ*, 336, 606
Crusius, A., & Schlickeiser, R. 1986, *A&A*, 164, L16
Fanti, C., Pozzi, F., Fanti, R., et al. 2000, *A&A*, 358, 499
Haas, M., Klaas, U., Müller, S., et al. 2003, *A&A*, 402, 87
Haas, M., Müller, S., Bertoldi, F., et al. 2004, *A&A*, 424, 531
Haas, M., Siebenmorgen, R., Schulz, B., Krügel, E., & Chini, R. 2005, *A&A*, submitted
Kreysa, E., Gemünd, H.-P., Gromke, J., et al. 1998, *SPIE*, 3357, 319
Lawrence, A. 1991, *MNRAS*, 252, 586
Marscher, A. P. 1977, *ApJ*, 216, 244
Meisenheimer, K., Haas, M., Müller, S., et al. 2001, *A&A*, 372, 719
Orr, M., & Browne, I. 1982, *MNRAS*, 200, 1067
Pacholzyk, A. 1970, *Radio astrophysics* (San Francisco: W.H. Freeman & Comp)
Simpson, C. 2005, *MNRAS*, 360, 565
van Bemmell, I., & Bertoldi, F. 2001, *A&A*, 368, 414
Willott, C., Rawlings, S., Archibald, E., et al. 2002, *MNRAS*, 331, 435